Short communication

Highly durable and active non-precious air cathode catalyst for zinc air battery

Zhu Chen[a], Ja-Yeon Choi[a], Haijiang Wang[b], Hui Li[b], Zhongwei Chen[a],*

[a] Department of Chemical Engineering, Waterloo Institute for Nanotechnology, Waterloo Institute for Sustainable Energy, University of Waterloo, Waterloo, ON, Canada, N2L 3G1
[b] Institute for Fuel Cell Innovation, National Research Council Canada, 4250 Wesbrook Mall, Vancouver, BC, Canada, V6T 1W5

ARTICLE INFO

ABSTRACT

The electrochemical stability of non-precious FeCo-EDA and commercial Pt/C cathode catalysts for zinc air battery have been compared using accelerated degradation test (ADT) in alkaline condition. Outstanding oxygen reduction reaction (ORR) stability of the FeCo-EDA catalyst was observed compared with the commercial Pt/C catalyst. The FeCo-EDA catalyst retained 80% of the initial mass activity for ORR whereas the commercial Pt/C catalyst retained only 32% of the initial mass activity after ADT. Additionally, the FeCo-EDA catalyst exhibited a nearly three times higher mass activity compared to that of the commercial Pt/C catalyst after ADT. Furthermore, single cell test of the FeCo-EDA and Pt/C catalysts was performed where both catalysts exhibited pseudolinear behaviour in the 12–500 mA cm^{-2} range. In addition, 67% higher peak power density was observed from the FeCo-EDA catalyst compared with commercial Pt/C. Based on the half cell and single cell tests the non-precious FeCo-EDA catalyst is a very promising ORR electrocatalyst for zinc air battery.

1. Introduction

Zinc air battery is a very promising technology owing to the potential benefits, including cost-effective design, high energy density, easy fuel storage, non-flammable and non-explosive nature, as well as facile reaction kinetics at the zinc electrode [1,2]. Acute international awareness has generated keen interest in the development of zinc air batteries as an integral part of sustainable energy systems for the future. In order to deliver a long-standing promise of becoming an efficient and commercially viable source of clean energy, zinc air batteries need to overcome formidable technical and economic challenges. One of these challenges is the air cathode catalyst which limits the cost, performance and life-time of zinc air batteries [3]. At present, the most effective oxygen reduction reaction (ORR) catalyst for the cathode of zinc air batteries is Pt, Pt–Ru alloys and oxides. However these catalysts are expensive and suffer considerable degradation via different pathways such as platinum particle agglomeration [4,5], detachment [6–8] and poisoning [9]. Non-precious metal catalysts (NPMCs) including organometallic compounds [10] and mixed metal oxides with perovskite [11], or spinel [12] structures have been studied extensively. However, the requirement for the commercialization of zinc air battery could not be met based on the current state of activity and durability of these NPMCs. Consequently, the development of highly active, stable, and affordable ORR catalyst is a critical issue.

A class of NPMC based on nitrogen chelated iron or cobalt carbon material was found to be a potential ORR catalyst for zinc air battery owing to the high ORR activity in alkaline conditions [13,14]. However, evaluation of the stability of this class of NPMC and the study of degradation mechanism are required for a complete understanding of the underlying catalytic principles. Furthermore, only half cell ORR activity was frequently reported for this catalyst, which is not an accurate representation of the operation of a real zinc air battery. In this paper, we pioneer the study of an ORR catalyst prepared by high temperature pyrolysis using from iron, cobalt, and ethylenediamine (FeCo-EDA). The ORR performance of the in-house FeCo-EDA catalyst was evaluated by a single cell setup in alkaline condition in addition to a half cell setup to achieve a more realistic cell operation environment. Additionally, the stability of the in-house FeCo-EDA catalyst was evaluated in a half cell setup and the degradation mechanism was examined briefly. The results of the in-house catalyst were compared with that of the commercial Pt/C to assess the potential use of FeCo-EDA as the cathode catalyst for zinc air battery.

2. Experimental methods

Commercial Pt/C catalyst obtained from BASF Fuel Cell Inc. was used for the half cell and single cell tests. The FeCo-EDA catalyst was prepared by high temperature pyrolysis [15]. Briefly, 0.25 g of iron sulphate and cobalt nitrates were dissolved in 125 mL of ethanol

* Corresponding author. Tel.: +1 519 888 4567x38664; fax: +1 519 746 4979.
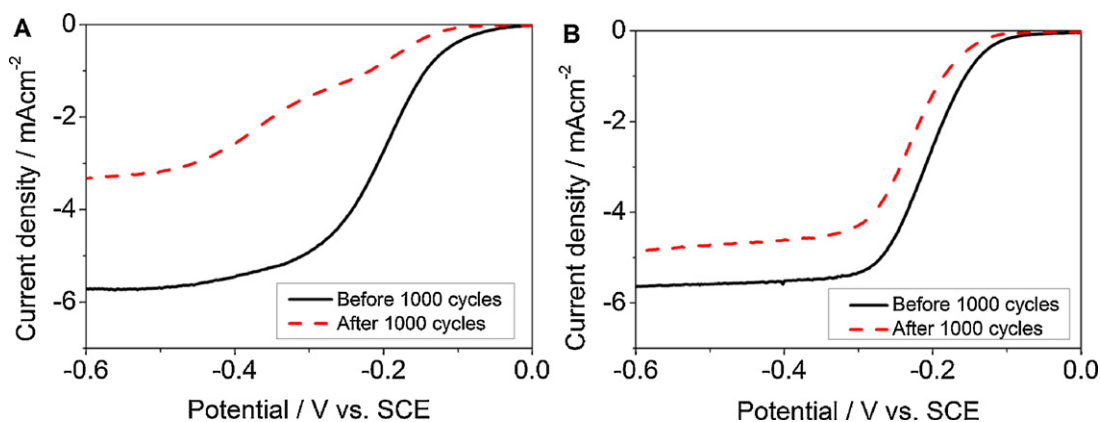E-mail address: zhwchen@uwaterloo.ca (Z. Chen).

Fig. 1. ORR polarization curve of (A) Pt/C and (B) FeCo-EDA before and after ADT.

followed by addition of 2 mL of ethylenediamine and 0.5 g of pre-treated carbon support. The materials were refluxed at 80 °C and pyrolyzed at 900 °C for 1 h in nitrogen gas. The obtained product was treated in 0.5 M H_2SO_4 for 8 h and washed before durability test.

To characterize the Pt/C and FeCo-EDA catalysts, transmission electron microscopy (TEM) (PHILIPS, CM300) was used to examine the surface microstructures. X-ray photoelectron spectroscopy (XPS) (Thermal Scientific, K-Alpha XPS spectrometer) was used to study the surface nitrogen group of the catalysts. The electrocatalytic activity and stability of the catalyst samples were measured using RDE voltammetry system which consisted of a potentiostat (eDAQ, ED210) and a rotation speed controller (Pine Instrument Co., AFMSRCE).

Prior to the RDE voltammetry, the catalyst ink was prepared by suspending 4 mg of catalyst in 2 mL of 0.2 wt.% Nafion solution. The glassy carbon area of the working electrode was deposited with 20 μL of ink. Once the ink dried, the working electrode was immersed into a glass cell containing 0.1 M of potassium hydroxide. A double junction saturated calomel electrode and a platinum wire were inserted into the electrolyte to serve as the reference electrode and counter electrode respectively. The temperature of the electrolyte solution was maintained at 50 °C during the course of experiment to accelerate the degradation of catalysts which was carried out in N_2 saturated electrolyte solution. The potential range of the accelerated degradation test (ADT) was swept from −1 to 0.2 V vs. SCE at a scan rate of 50 mV s^{-1}. The capacitive current was measured by cyclic voltammetry (CV) in N_2 saturated electrolyte solution. The potential range of CV experiment was from −1 to 0.2 V vs. SCE with a scan rate of 50 mV s^{-1}. The ORR was performed in O_2 saturated electrolyte solution in the same potential window under various rotation speeds at a scan rate of 10 mV s^{-1}.

Single cell test of the catalyst was performed using a multichannel potentiostat (Princeton Applied Research, VersaSTAT MC) and a home-made zinc air battery. A polished zinc plate and a piece of catalyst coated gas diffusion layer (Ion Power Inc., SGL Carbon 10 BB, 2.5 cm × 2.5 cm) were used at anode and cathode respectively. The catalyst loading on the gas diffusion layer was 1.5 mg$_{catalyst}$ cm^{-2} and the electrolyte used in the zinc air battery was 6 M KOH. Galvanodynamic method was used to discharge the single cell from 0 to 500 mA cm^{-2}. Open circuit voltage of the single cell was also determined by measuring the stabilized potential difference between the cathode and the anode.

3. Results and discussion

Severe degradation of the Pt/C catalyst compared with FeCo-EDA is showed by the decrease in the ORR performance. At −0.3 V

vs. SCE, the mass activity of the Pt/C and FeCo-EDA catalysts before the ADT is 24.1 and 26.2 mA mg^{-1} respectively. After ADT, the FeCo-EDA catalyst retained 80% (21.0 mA mg^{-1}) of the initial mass activity whereas the Pt/C catalyst retained only 32% (7.8 mA mg^{-1}) of the initial mass activity. From the ORR polarization curves (Fig. 1A), the decrease in onset potential, half wave potential and limiting current density was 0.05 V, 0.112 V and 2.4 mA cm^{-2} respectively in the case of Pt/C catalyst. The decrease in onset, half wave and limiting current density is 0.05 V, 0.022 V and 0.8 mA cm^{-2} respectively in the case of FeCo-EDA. Similar decrease in the onset potential is observed for both catalysts, however with respect to half wave potential and limiting current density, the Pt/C catalyst showed respectively, five and four times greater degradation compared to FeCo-EDA catalyst. Comparing these results, much lower degradation was observed for the FeCo-EDA catalyst (Fig. 1B).

The great potential of FeCo-EDA material as a catalyst for the ORR in zinc air battery can be further supported by the results of single cell test shown in Fig. 2. From the polarization curve, FeCo-EDA exhibited current density of 261 mA cm^{-2} which is significantly higher compared with the current density of 196 mA cm^{-2} obtained by Pt/C at 0.8 V. Additionally, much higher peak power density was observed for FeCo-EDA (232 mW cm^{-2}) compared with Pt/C (139 mW cm^{-2}). Furthermore, the ohmic overpotential was a dominant performance loss mechanism in the region between 15 and 500 mA cm^{-2} for both catalysts based on the observed pseudolinear behaviour from the polarization curve.

Koutecky–Levich (K–L) plots for ORR at −0.4 and −0.5 V vs. SCE before and after ADT were constructed for the Pt/C catalyst (Fig. 3A and C). The increase in the slope of the K–L plot after ADT suggests a decrease in the number of electrons transferred in the oxygen reduction process. By extrapolation of K–L plot to the y axis, the kinetic current density before and after ADT for Pt/C is 49 and 12 mA cm^{-2} respectively at −0.5 V. In the case of FeCo-EDA, the slope of K–L plot before and after ADT showed very little change indicating little variation with respect to the number of electrons transferred in the reduction process (Fig. 3B and D). The kinetic current density obtained in a similar manner from the K–L plots is 50 and 29 mA cm^{-2} before and after cycling respectively. Once more, the FeCo-EDA out-performs the commercial Pt/C catalyst in terms of the kinetic current density where more than 50% was retained for FeCo-EDA after ADT. The observed electrochemical performances clearly demonstrate that the FeCo-EDA is a more suitable ORR catalyst for zinc air battery.

TEM was used to study the morphological changes of the catalysts which are commonly associated with degradation. For the Pt/C catalyst, significant morphology change was demonstrated by the TEM image (Fig. 4A and B) before and after ADT. Prior to
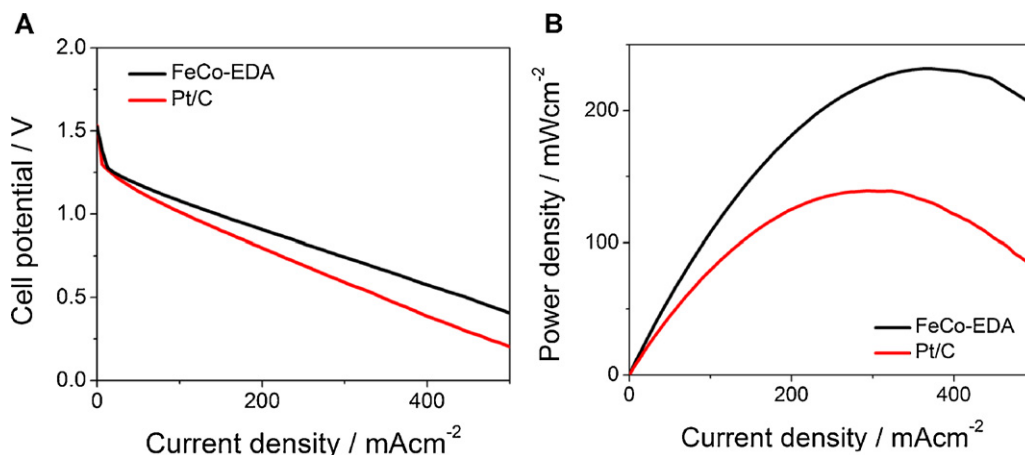
Fig. 2. Single cell performance of the zinc air battery showing (A) polarization curve and (B) power density.

ADT, the average size of platinum nanoparticle is 3.85 ± 0.92 nm showing a narrow size distribution—a property desirable for catalysts. After cycling, significant increase in the size of platinum particle and an increase in the particle size distribution is evident showing an average particle size of 9.13 ± 5.7 nm. Agglomeration of platinum particles is a widely observed phenomenon in Pt/C degradation testing and it has been attributed to be an important factor for Pt/C performance degradation in many studies [16,6]. To the contrary, higher stability of the FeCo-EDA catalyst can be attributed to the stable catalyst structure observed from TEM where no obvious morphology change was observed (Fig. 4C and D). Nitrogen content of the FeCo-EDA catalyst was determined using XPS (Fig. 5A) which illustrated change in the overall nitrogen content before (2.18 at.%) and after (1.55 at.%) ADT. Based on the high resolution N 1s spectra (Fig. 5B), pyridone, pyrrolic/quaternary and pyridinic nitrogen groups are present in the FeCo-EDA catalyst. The FeCo-EDA catalyst demonstrated 23.5% and 27.9% decrease in the quaternary/pyrrolic and pyridinic nitrogen group respectively after ADT. Although the exact catalytic identity of the nitrogen groups are debatable, these apparent changes in the nitrogen groups could cause the slight decrease in ORR performance of the FeCo-EDA catalyst since the pyridinic and quaternary nitrogen groups are believed to be important in ORR catalysis for NPMCs [17]. Additionally, similar profile of the N 1s signal was observed before and after ADT which could partially explain the higher stability of the FeCo-EDA catalyst.

Based on the CV voltammogram of the Pt/C catalyst (Fig. 6A), only 22% of the initial ECSA values remained after ADT, which suggests possible contribution of platinum detachment to the degradation mechanisms in addition to particle agglomeration.
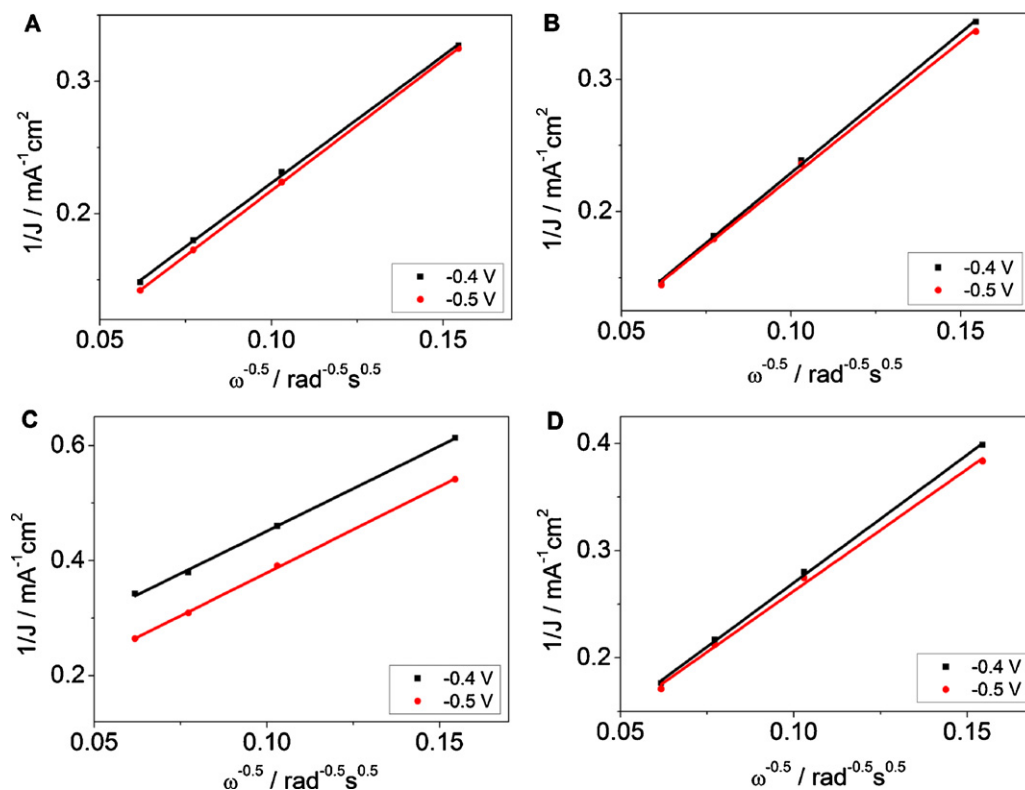

Fig. 3. Koutecky–Levich plot of (A) Pt/C and (B) FeCo-EDA before ADT. Koutecky–Levich plot of (C) Pt/C and (D) FeCo-EDA after ADT.
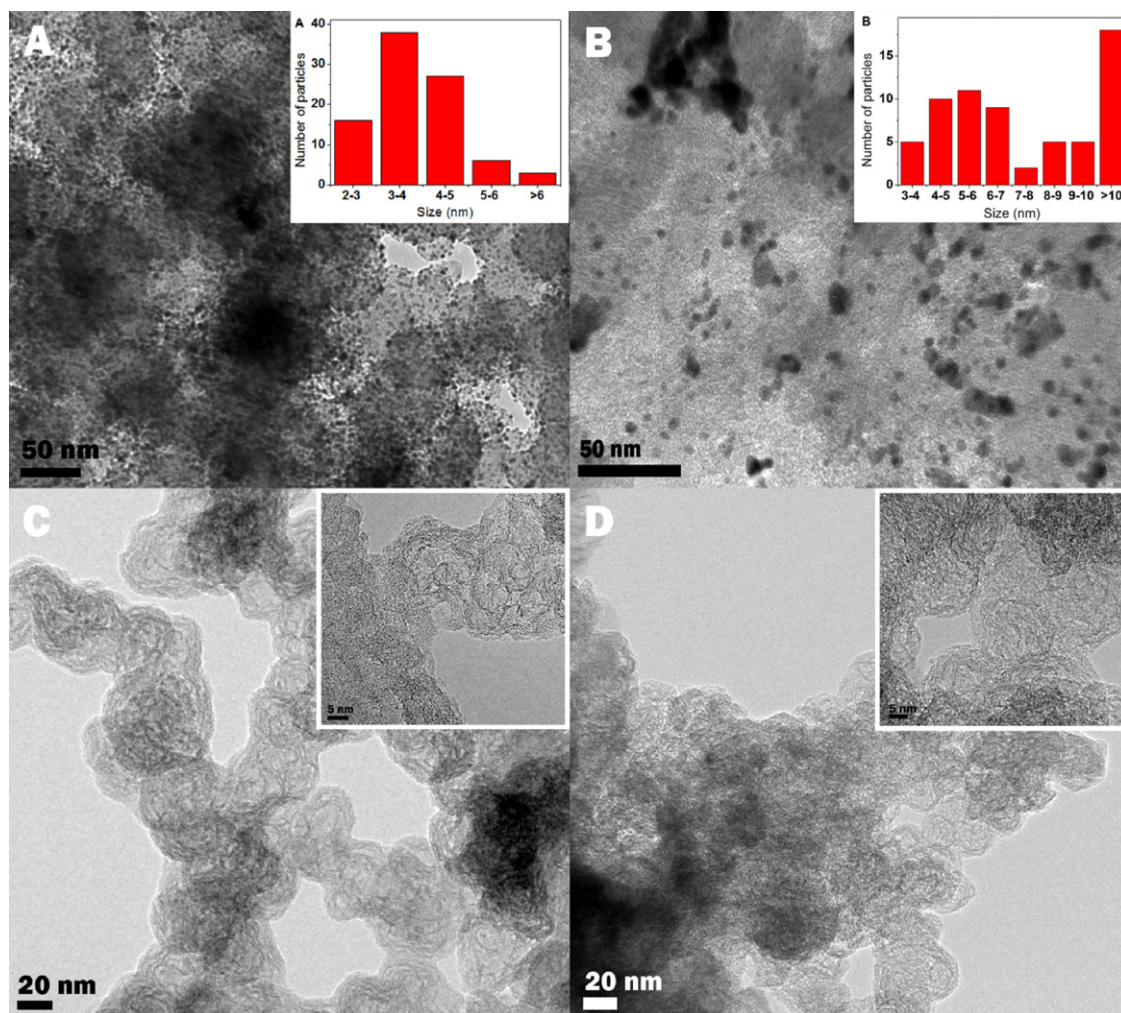
Fig. 4. TEM image of Pt/C catalyst (A) before and (B) after ADT in 0.1 M KOH at 50 °C. Inset of (A) and (B) showing the size distribution of platinum particles. TEM image of FeCo-EDA catalyst (C) before and (D) after ADT, inset of (C) and (D) showing the higher resolution TEM image.

Similar platinum detachment from carbon support into the electrolyte without re-deposition has been observed [18] and it has been attributed to be the predominant degradation mechanism. The small current plateau near −0.36 V vs. SCE in Fig. 1A could be attributed to the oxygen reduction catalysis by carbon materials. Previous works have investigated the effect of carbon material and platinum loading on the oxygen reduction behaviours of Pt/C [19,20]. Based on these studies, carbon could contribute to oxygen reduction at potentials lower than 0.7 V vs. RHE especially for

low platinum loading [21]. As a result, after ADT ORR by carbon could be more renounced as the platinum loading was lowered by either particle agglomeration or platinum dettachment. In contrast, the CV voltammogram (Fig. 6B) of FeCo-EDA only showed slight decrease in the capacitance—70 F g^{-1} before ADT and 57 F g^{-1} after ADT. Capacitance of non precious metal catalyst based on carbon could be related to the active site groups and the decrease in the capacitance could suggest the disappearance of unstable active site groups.
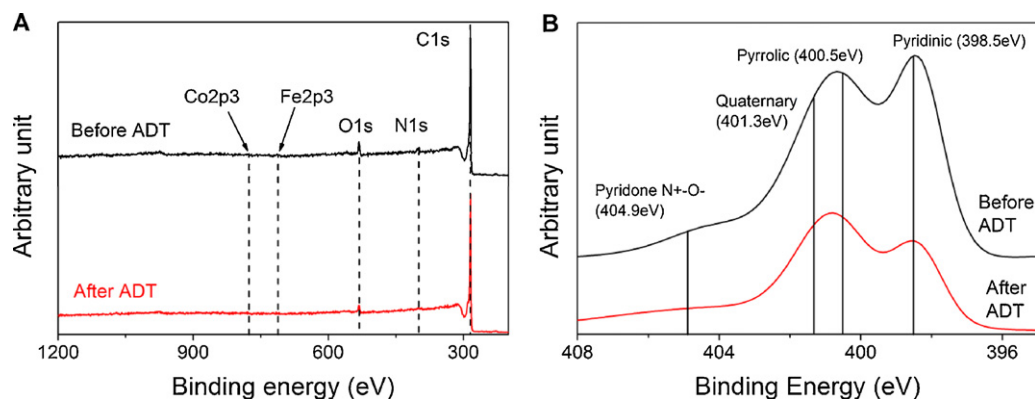

Fig. 5. XPS spectrum of FeCo-EDA catalyst before and after ADT: (A) full survey spectrum and (B) high resolution N 1s spectrum.
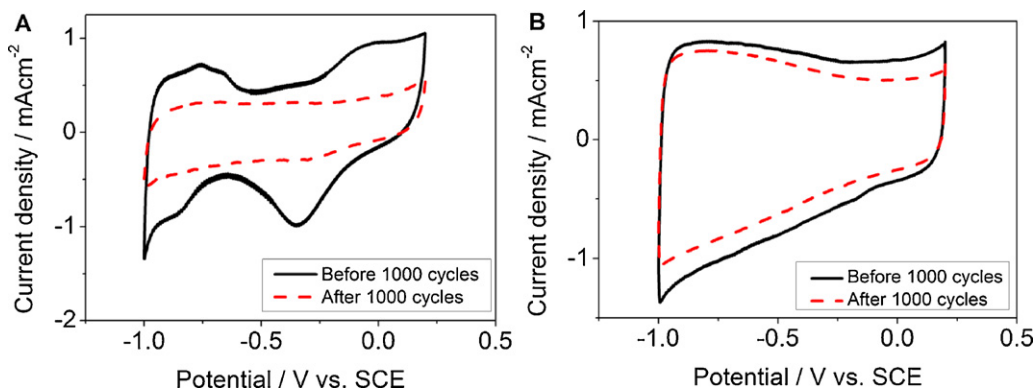
Fig. 6. CV voltammogram of (A) Pt/C and (B) FeCo-EDA before and after ADT.

4. Conclusion

In this study evaluation of ORR activity of FeCo-EDA catalyst and Pt/C catalysts has been examined in alkaline condition by half cell and single cell tests. The FeCo-EDA catalyst exhibited superior ORR activity in terms of better peak power density and mass activity. From the ADT, the FeCo-EDA catalyst retained a nearly three times higher mass activity compared to that of Pt/C catalyst. Results from the TEM and XPS characterization suggest the higher durability of FeCo-EDA can be originated from the stable morphological and chemical structures. The similar activity and much more superior stability of the FeCo-EDA catalyst can meet the high activity, stability and lower cost requirements of the ORR catalyst in zinc air battery.

Acknowledgements

References

[1] S.I. Smedley, X.G. Zhang, J. Power Sources 165 (2007) 897–904.
[2] P. Sapkota, H. Kim, J. Ind. Eng. Chem. 15 (2009) 445–450.
[3] V. Neburchilov, H. Wang, J.J. Martin, W. Qu, J. Power Sources 195 (2010) 1271–1291.
[4] R.L. Borup, J.R. Davey, F.H. Garzon, D.L. Wood, P.M. Welch, K. More, ECS Trans. 3 (2006) 879–886.
[5] S. Mitsushima, S. Kawahara, K. Ota, N. Kamiya, J. Electrochem. Soc. 154 (2007) B153–B158.
[6] K.T. Kim, Y.G. Kim, J.S. Chung, J. Electrochem. Soc. 142 (1995) 1531–1538.
[7] M. Watanabe, K. Tsurumi, T. Mizukami, T. Nakamura, P. Stonehart, J. Electrochem. Soc. 141 (1994) 2659–2668.
[8] W. Roh, J. Cho, H. Kim, J. Appl. Electrochem. 26 (1996) 623–630.
[9] S. Zhang, X.-Z. Yuan, J.N.C. Hin, H. Wang, K.A. Friedrich, M. Schulze, J. Power Sources 194 (2009) 588–600.
[10] A.L. Zhang, H. Wang, W. Qu, X. Li, Z. Jong, H. Li, J. Power Sources 195 (2010) 5587–5595.
[11] Y.-M. Chang, P.-W. Wu, C.-Y. Wu, Y.-C. Hsieh, J. Power Sources 189 (2009) 1003–1007.
[12] M. Hamdani, R.N. Singh, P. Chartier, Int. J. Electrochem. Sci. 5 (2010) 556–577.
[13] M. Lefèvre, E. Proietti, F. Jaouen, J.P. Dodelet, Science 324 (2009) 71–74.
[14] F. Jaouen, J.P. Dodelet, J. Chem. Phys. C 113 (2009) 15422–15432.
[15] J.Y. Choi, R.S. Hsu, Z. Chen, J. Phys. Chem. C 114 (2010) 8048–8053.
[16] A. Honji, T. Mori, K. Tamura, Y. Hishinuma, J. Electrochem. Soc. 135 (1988) 355–359.
[17] X. Li, G. Liu, B.N. Popov, J. Power Sources 195 (2010) 6373–6378.
[18] K.J.J. Mayrhofer, J.C. Meier, S.J. Ashton, G.K.H. Wiberg, F. Kraus, M. Hanzlik, M. Arenz, Electrochem. Commun. 10 (2008) 1144–1147.
[19] J. Perez, A.A. Tanaka, E.R. Gonzalez, E.A. Ticianelli, J. Electrochem. Soc. 141 (1994) 431–436.
[20] J. Perez, E.R. Gonzalez, E.A. Ticianelli, Electrochem. Acta 44 (1998) 1329–1339.
[21] J.S. Spendelow, A. Wieckowski, Phys. Chem. Chem. Phys. 9 (2007) 2654–2675.